Chaotic behavior of the radiation field in the magnetically insulated transmission line oscillator

Hao Jianhong[1,2] and Ding Wu[3]
[1]*Department of Physics, Shijiazhuang Teacher's College, Shijiazhuang 050801, China*
[2]*Graduate School, China Academy of Engineering Physics, P.O. Box 2101, Beijing 100088, China*
[3]*Institute of Applied Physics and Computational Mathematics, P.O. Box 8009, Beijing 100088, China*
(Received 19 July 2002; published 27 February 2003)

In terms of the nonlinear coupled equations that describe the evolution of the radiation field and electrons motion in the magnetically insulated transmission line oscillator, the nonlinear instabilities existing in the process of the interaction between the electron beam and field are analyzed. It is shown that the development of the instability leads to the appearance of the nonlinear behavior of the radiation field. (1) In the soft nonlinear regime in which the radiation field is characterized by the periodic limit cycle, the power spectrum is discrete and the sideband is not symmetric around the carrier frequency; in the hard nonlinear regime in which the radiation field is characterized by the chaotic oscillation, the power spectrum is continuous and the spectral components with larger amplitude distribute in the low frequency region. (2) The threshold current at which the limit cycle or chaotic oscillation starts occurring is a function of the detuning. The appearance of the nonlinear unsteady states may be accelerated and inhibited by controlling detuning. (3) The arising of the limit cycle oscillation and chaotic behavior of the radiation field is easier in a magnetically insulated transmission line oscillator than in a traveling wave tube amplifier.

DOI: 10.1103/PhysRevE.67.026503 PACS number(s): 52.59.Px, 41.75.Fr, 52.35.−g, 84.30.Le

I. INTRODUCTION

The magnetically insulated transmission line oscillator (MILO) is a crossed-field microwave device with a power level of GW. Two distinguished features of the MILO from other microwave devices are the following.

(1) The dc magnetic field, which combines with an orthogonal dc electric field to determine the electron drift velocity, is generated by the intrinsic electron current in the device. Consequently, there is no need for an external dc magnetic field.

(2) The dc magnetic field in the MILO prevents electrons emitted on the cathode from reaching the anode.

This self-insulating property inhibits electrical breakdown of the anode-cathode gap, which enables the tube to handle extremely large input and output power. The peak power of 1.5 GW and microwave energy of 300 J at *L* band have been achieved [1]. As other high power relativistic microwave devices, the MILO ordinarily operates in extremely nonlinear regime so that the intrinsic nonlinear effects of the nonlinear system, such as the limit cycle and chaotic oscillation of the field, may occur. The chaotic behavior directly affects the output characteristic such as the efficiency and bandwidth etc. Therefore, the study of the chaotic phenomenon is significant for theory and practice. In this aspect, there have been a number of successful works for the free electron laser (FEL) [2–7] and some investigations for high power microwave devices as well [8,9]. In this paper, the limit cycle and chaotic behaviors of the radiation field in the MILO are simulated and discussed.

II. BASIC THEORY

In this section, we present a basic model of the interaction between electrons and the radiation field in the MILO. In analysis we consider that (1) the MILO is a system with cylindrical symmetry, (2) the electron motion is predominantly axially drifting (parallel to z axis), $v_z = c(E_{r0}/B_{\theta 0} + E_r/B_{\theta 0})$, where $B_{\theta 0}$ is the angular component of the self-insulating dc magnetic field generated by all currents, E_{r0} and E_r are the radial components of the dc electric field and ac electric field in the diode, respectively.

The electromagnetic field in a MILO can be expressed in the following form:

$$\mathbf{E} = [\mathbf{E}_p(r)\varepsilon(z,t) + \mathbf{E}^{(s)}(r,z,t)]\exp[i(kz-\omega t)] + \text{c.c.},$$
$$\mathbf{B} = [\mathbf{B}_p(r)\varepsilon(z,t) + \mathbf{B}^{(s)}(r,z,t)]\exp[i(kz-\omega t)] + \text{c.c.} \quad (1)$$

On the right-hand side of the above equations, the first term is the radiation field and the second term is the space charge wave field which can be expressed as [10]

$$\mathbf{E}^{(s)}(r,z,t) = -\frac{4\pi\mu}{\epsilon}\mathbf{E}^{(r)} = -\frac{4\pi\mu}{\epsilon}\mathbf{E}_p(r)\varepsilon(z,t), \quad (2)$$

where μ and ϵ are magnetic conductivity and dielectric constant of the space charge wave, respectively. ε is the slowly varying complex amplitude of the radiation field and its evolution equation is given by [8]

$$\frac{\partial\varepsilon}{\partial t} + v_g\frac{\partial\varepsilon}{\partial z} = -\frac{Id}{u}E^*_{pz}(r_b)\langle\exp(-i\phi_j)\rangle, \quad (3)$$

where u is the electromagnetic energy per $|\varepsilon|^2$ contained in one period, v_g is the group velocity for the vacuum electromagnetic wave, d is the period of the structure, r_b is beam radius, I is the local beam current passing a particular point which equals the beam current emitted to the interaction region on the cathode.

As an electron travels down the interaction region, its phase evolves according to

$$\frac{d\phi_j}{dt}=\frac{\partial\phi_j}{\partial t}+v_g\frac{\partial\phi_j}{\partial z}=kv_{jz}-\omega, \tag{4}$$

where $v_{jz}=v_{z0}+\Delta v_{jz}$, $v_{z0}=cE_{r0}/B_{\theta 0}$, Δv_{jz} is the drift velocity incited by the radiation field E_r and it can be given by

$$\Delta\beta_{jz}=\frac{\Delta v_{jz}}{c}=\frac{E_{pr}}{B_{\theta 0}}\left(1-\frac{4\pi\mu}{\epsilon}\right)\varepsilon\exp(i\phi_j)+\text{c.c.} \tag{5}$$

Using the Lagrangian time coordinate $t=t_0+\int_0^z dz'[1/v_{jz}(t_0,z')]$, Eqs. (3) and (4) become

$$\alpha_j\left(1-\frac{v_g}{v_{jz}}\right)\frac{\partial\varepsilon}{\partial t_0}+v_g\frac{\partial\varepsilon}{\partial z}=-\frac{Id}{u}E_{pz}^*\langle\exp(-i\phi_j)\rangle, \tag{6}$$

$$\frac{\partial\phi_j}{\partial z}=\Delta k+\frac{\omega}{c}\frac{\Delta\beta_{jz}}{\beta_{z0}^2}, \tag{7}$$

where

$$\alpha_j^{-1}=1+\int_0^z dz'\frac{\partial}{\partial t_0}v_{jz}^{-1}(z',t_0),$$

$\Delta k=k-\omega/v_{z0}$ is the detuning. In calculation, we set $\alpha_j\approx 1$ and $v_{jz}\approx v_{z0}$ to satisfy that the slowly varying amplitude ε is independent of the phase of any particular electron. This assumption is valid under the circumstances: (1) The fields are stationary in time. (2) If the efficiency in a pass is poor, or if the electron motion is ultrarelativistic ($v_{jz}\approx c$), then all electrons have nearly same velocity which is equal to the injected velocity when they traverse the interaction region [8] (MILO satisfies the condition).

Introducing the normalized axial distance

$$\zeta=z'/L, \tag{8}$$

the normalized time

$$\tau=v_g t_0/L, \tag{9}$$

the normalized field amplitude

$$a=\frac{E_{pr}}{B_{\theta 0}}\left(1-\frac{4\pi\mu}{\epsilon}\right)\varepsilon, \tag{10}$$

and the universal current, which is a dimensionless quantity

$$\tilde{I}=I\frac{dLE_{pz}^*E_{pr}}{uv_gB_{\theta 0}}\left(1-\frac{4\pi\mu}{\epsilon}\right), \tag{11}$$

where L is the length of the interaction region. Then Eqs. (5)–(7) become

$$\left(1-\frac{v_g}{v_{z0}}\right)\frac{\partial a}{\partial\tau}+\frac{\partial a}{\partial\zeta}=-\tilde{I}\langle\exp(-i\phi_j)\rangle, \tag{12}$$

$$\frac{\partial\phi_j}{\partial\zeta}=L\Delta k+L\frac{\omega}{c}\frac{\Delta\beta_{jz}}{\beta_{z0}^2}, \tag{13}$$

$$\Delta\beta_{jz}=a\exp(i\phi_j)+\text{c.c.} \tag{14}$$

Clearly, Eqs. (12)–(14) are the nonlinear equations that describe the interaction between the radiation field and the electrons. Simple manipulation of Eqs. (12) and (14) yields a conservation equation

$$\left(1-\frac{v_g}{v_{z0}}\right)\frac{\partial|a|^2}{\partial\tau}+\frac{\partial}{\partial\zeta}|a|^2+\tilde{I}\langle\Delta\beta_{jz}\rangle=0. \tag{15}$$

III. THE INSTABILITY AND THRESHOLD

The starting current which is the minimum beam current required from noise to start oscillation is considered as a scale of the current injected to the interaction region, and it can be determined by numerical calculation [11].

An oscillator can be considered as an amplifier to be analyzed, thus we choose the normalized length $L\omega/c=1600$ and the normalized injected velocity $\beta_{z0}=0.86$ (corresponding to diode voltage of 500 kV) with consideration of the fact that actual radiation field reaches a saturation state in several tens of nanoseconds and using the parameters in Refs. [12,13]. Considering the wave-particle interaction and the radiation field propagation, we choose the normalized group velocity $\beta_g=0.24$. In addition, it is assumed that the duration of the beam pulse in the simulation is long enough, so that evolution equations involve only two parameters: the ratio of the beam current to the starting current $\chi=I/I_{st}$ and detuning Δk.

The universal current as a ''source'' term of the amplitude evolution equation has the most important effect on the behavior of the radiation field and its magnitude determines the operating state of the device. For very small χ, the output power oscillates regularly as the current changes; for large χ, the device operates in the nonlinear chaotic regime, output power is very sensitive to the current change, and the oscillation becomes irregular with a number of spikes of high peak intensity as shown in Fig. 1. The numerical simulation shows the following: it is in the region of the spiking appearance that the system loses the stability and the nonlinear instability occurs. The nonlinear behaviors include the periodic oscillations [see Figs. 2(b) and 2(c)] with the threshold value χ_{cr1} and the arbitrary oscillations [see Fig. 2(d)] with the threshold value χ_{cr2}. The threshold value χ_{cr} is not a monotonous function of the detuning.

The purpose of the present study is to analyze the long time behavior of the nonlinear system, and Fig. 3 gives the spatial distribution of the radiation field in a long time. The field reaches saturation rapidly [see Fig. 3(a)] when the current is smaller. As the current increases, the radiation field is modulated in space around a saturation state level [see Fig. 3(b)] and can jump suddenly to another higher modulated level than the primary saturation level [see Fig. 3(c)]. The modulation is relatively strong for larger current [see Fig. 3(d)].

Reference [9] has studied the feedback between the input

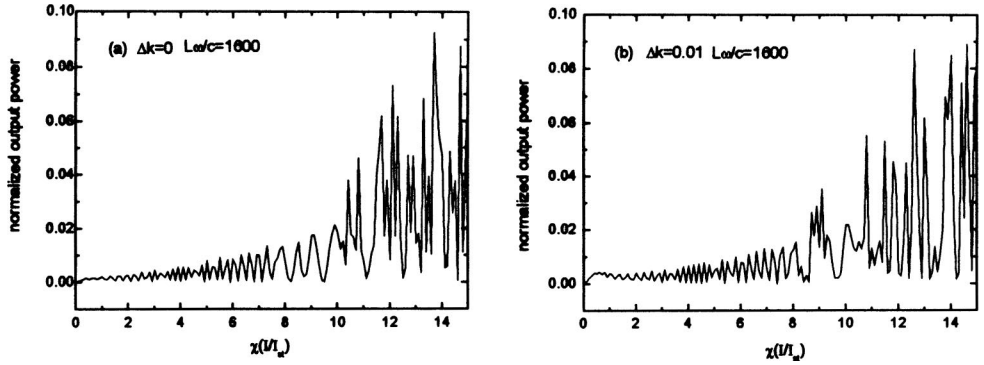

FIG. 1. The normalized output power vs the rate of the beam current to starting current with (a) $\Delta k=0$ and (b) $\Delta k=0.01$.

and output in the crossed-field devices; it shows that the development of the chaotic output patterns is connected with slow, large-amplitude hub density oscillations. The multimode excitation is also an instability generation mechanism [8]. Actually, the electromagnetic field of any RF structure may be represented by a superposition of a number of longitudinal eigenmodes. When the MILO operates in large current regime, some low-amplitude modes are excited, except the dominant mode, due to self-modulation instability, and in the FEL literature this instability is called the sideband instability. The progress of the sideband instability leads to the chaotic field appearing. In addition, the modes' competition induces cross-excitation instability, the energy exchange between the field and the electron or space charge effect causes overbunch instability, etc. The development of these instabilities may lead to the chaotic behaviors of the field.

IV. LIMIT CYCLE AND CHAOTIC OSCILLATION

The current dominates the evolution of the radiation field. The radiation field evolves from a steady saturation state to a limit cycle and eventually to a chaotic oscillation state as the current increases, this course is illustrated in Fig. 2. For a smaller χ, the output power grows and reaches the saturation [see Fig. 2(a)]. As the χ increases, the periodic solution of the system appears near χ_{cr1} and the radiation field exhibits the limit cycle oscillation. It is revealed that the system has lost its stability and undergone the Hopf bifurcation, the

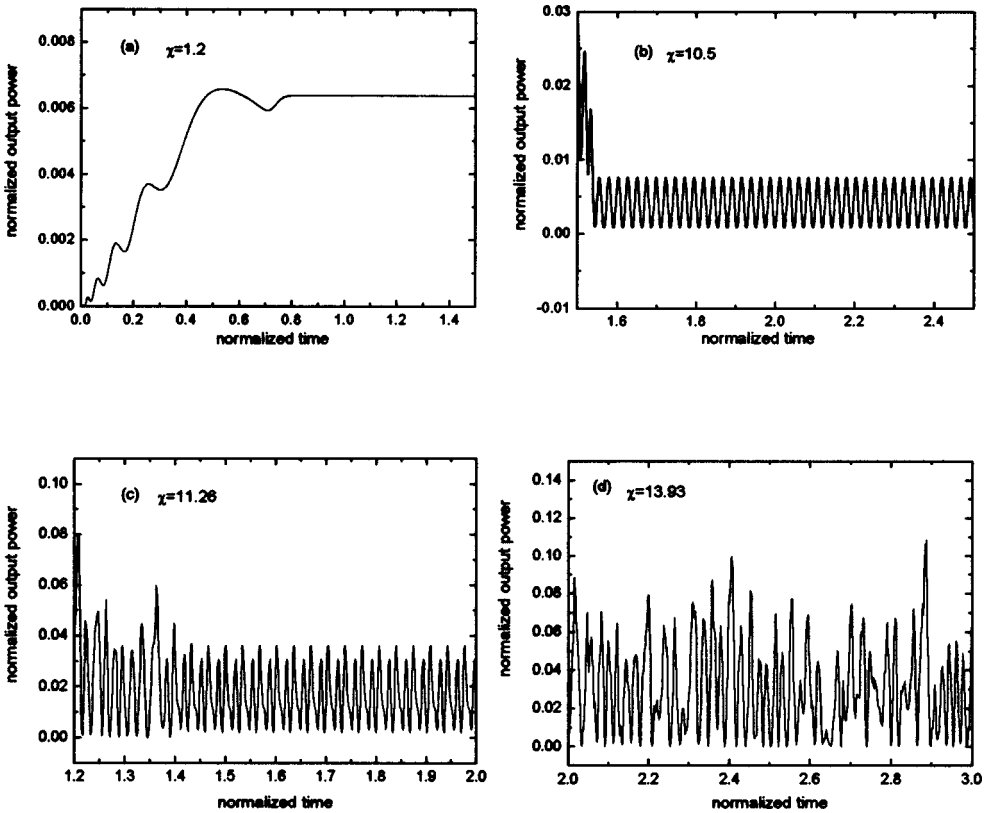

FIG. 2. The temporal evolution of the output power with $\Delta k=0$ for different currents.

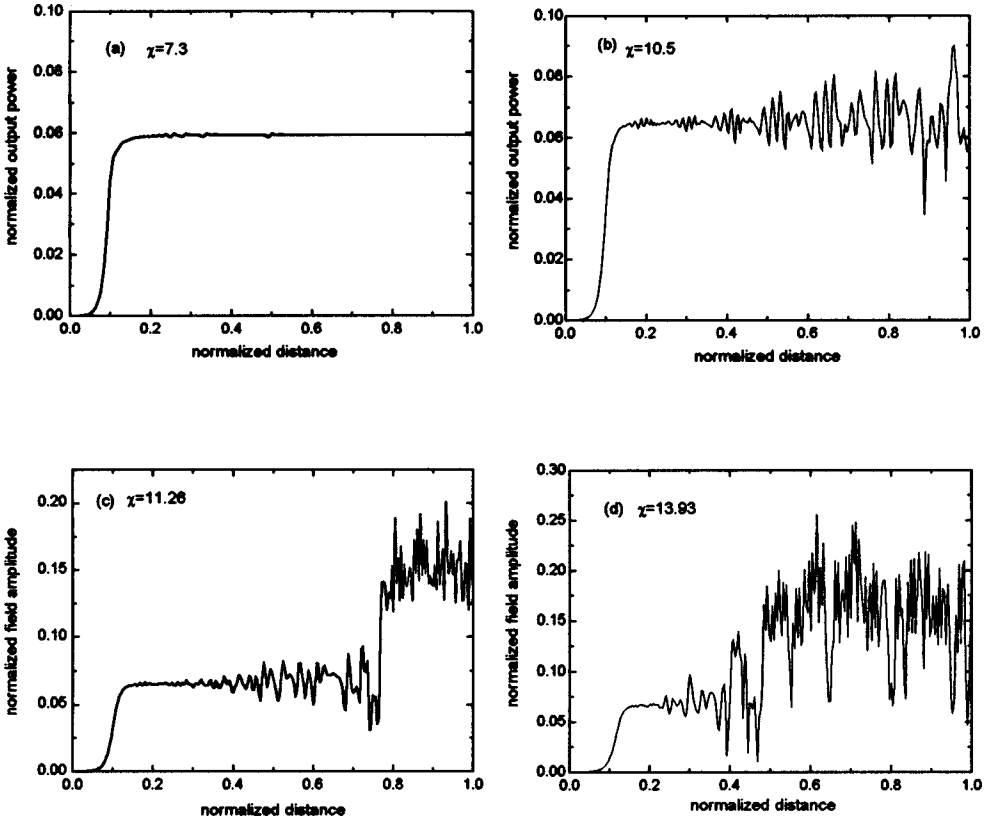

FIG. 3. The normalized field vs the normalized distance for different currents with $\Delta k=0$ and $\tau=3$.

single-frequency oscillation is destroyed and replaced by ensuing multifrequency oscillation as illustrated in Figs. 2(b) and 2(c); the chaotic solution of the system appears near χ_{cr2} and the radiation field exhibits the chaotic oscillation as illustrated in Fig. 2(d). It is found easily that the evolution of the radiation field in the MILO is a typical course of the period doubled bifurcation to chaos.

We call the region in which a periodic limit cycle appears as ''soft'' nonlinear regime, while the region at which a chaotic oscillation appears as ''hard'' nonlinear regime [14]. In the soft nonlinear regime of $\chi \geqslant \chi_{cr1}$, the radiation field characterizes the limit cycle oscillation and this oscillation state is intermittent but very dense. The output power spectrum is discrete and not symmetric relative to the carrier frequency [see Figs. 4(a) and 4(b)]; in the hard nonlinear regime of $\chi \geqslant \chi_{cr2}$, the radiation field characterizes the chaotic oscillation and this chaotic state is continuous. The output power spectrum is continuous and the spectral components with larger amplitude distribute in the region of $\leqslant 20$ GHz [see Fig. 4(c)].

To examine the dependence of the chaotic behavior on the detuning, the temporal evolution of the output power and the corresponding spectral distribution for different detunings are shown in Fig. 5. It is manifested that the relation between frequency characteristic of the radiation field and detuning is complicated, the appearance of the limit cycle and chaotic states may be accelerated and inhibited by controlling the detuning properly. The coupled equations (12)–(14) indicate that, at a spatial location, the energy exchange between the field and electron depends on the detuning Δk and the radiation field a of the location, therefore the threshold value of the nonlinear instability can be altered by adjusting the detuning, thus the appearance of the limit cycle and chaotic state can be hastened and inhibited.

The MILO is slightly different from the traveling wave tube (TWT) amplifier in the chaotic behavior [15].

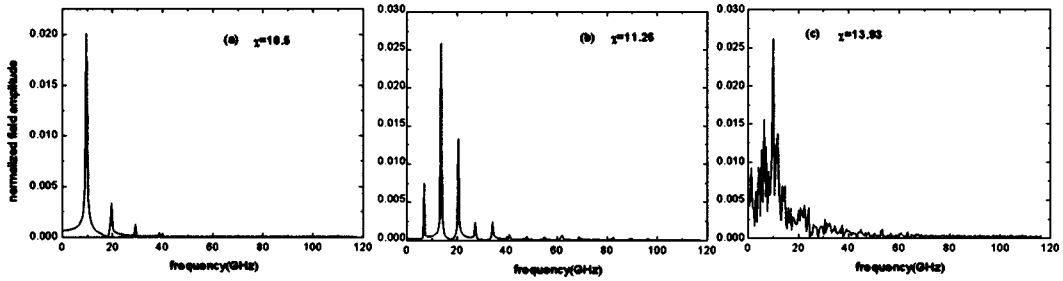

FIG. 4. The spectrum distribution of the normalized field with parameters in Figs. 2(b), 2(c), and 2(d).

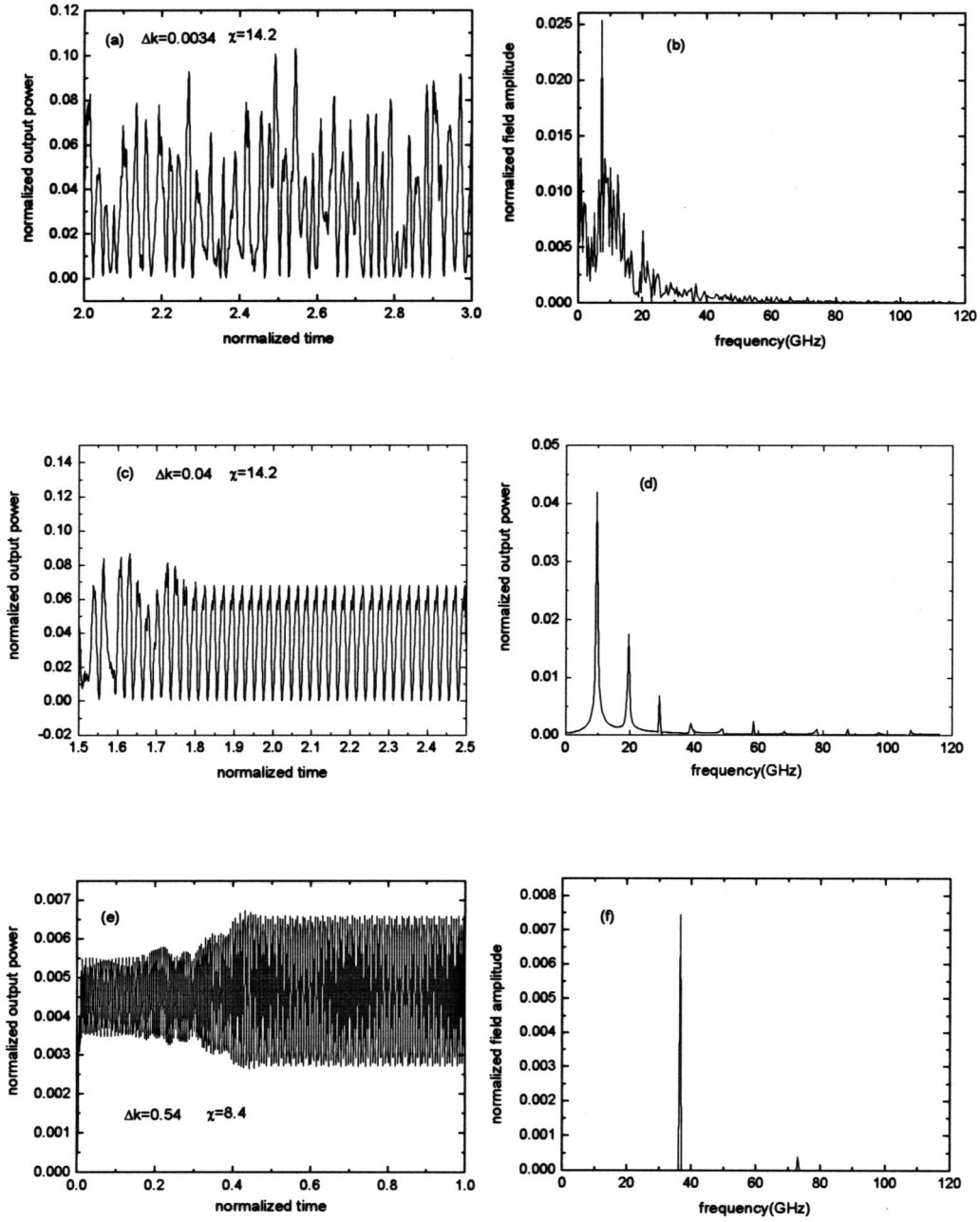

FIG. 5. The temporal evolution of the output power and corresponding spectral distribution for different detunings and currents.

(1) For the MILO, the threshold current of the limit cycle oscillation and chaotic state is smaller and the limit cycle appearance is relatively dense in the soft nonlinear regime. So the limit cycle and chaotic oscillation of the radiation field occur easily.

(2) The threshold current depends on the detuning for two devices, but the effect of the detuning on the threshold value only for the chaotic state is relatively striking in the TWT amplifier, while for the chaotic state and the limit cycle state, it is all more striking in the MILO.

This difference probably is the fact that the bunch mechanism is different for two devices. The TWT amplifier characterizes inertial bunching that includes two sets of the energy exchanging and dispersing and it is represented by double integral of the field. Whether the external action exists or not, this bunching will keep on developing; The MILO characterizes forced bunching which only includes one set of the phase modulation and it is represented by single integral of the field. Once the external field disappears, this bunching will end. The energy equation, for the TWT amplifier, is a differential equation

$$\frac{\partial(\Delta\beta_{jz}/\beta_{z0}^2)}{\partial z} = a_o \exp(i\phi_j) + \text{c.c.}, \tag{16}$$

and for the MILO, is an algebra equation

$$\Delta\beta_{jz} = a_m \exp(i\phi_j) + \text{c.c.} \tag{17}$$

In other words, the energy exchanging at a point in space, for the TWT amplifier, is proportional to spatial average of the radiation field amplitude and electrons phase over correlate range of this point; for the MILO, it is only proportional to the radiation field amplitude and electrons phase at this point. The electron bunching directly affects the energy exchanging between electrons and radiation field, so it finally influences the nonlinear behavior of the radiation field. Therefore, the behavior characteristic of the nonlinear instability and dependence of the threshold on the detuning are a little different for two devices.

V. CONCLUSION

Utilizing a set of nonlinear equations, which describes the interaction between the radiation field and electrons in the MILO, we analyze and simulate the limit cycle and chaotic oscillation of the field. The current χ and the detuning Δk are control parameters of the system, where the current is the dominant one. When the device operates in the chaotic regime of the large current, the output power becomes very low and a number of spikes appear in the curve of the output power with the current. In the parameter range, in which the curve becomes chaotic and irregular, the instability of the system leads to the limit cycle oscillation and chaotic behavior of the field occurring.

In the soft nonlinear regime of $\chi \geqslant \chi_{cr1}$, the radiation field exhibits discontinuous periodic limit cycle, which is characterized by the frequency bifurcation and discrete power spectrum; in the hard regime of $\chi \geqslant \chi_{cr2}$, the radiation field exhibits the continuous chaotic state, which is characterized by nonperiod of the radiation field in time and a wide continuous power spectrum. The threshold current (χ_{cr1}, χ_{cr2}) of the limit cycle and chaotic oscillation appearing is a function of the detuning (Δk). The limit cycle and chaotic behavior of the field can be accelerated and inhibited by optimizing the detuning properly.

ACKNOWLEDGMENTS

The authors are grateful to Professor Zhichou Zhang for helpful stimulated discussions. We also wish to thank Yunyuan Yang for helpful suggestions and discussions.

[1] M. Haworth *et al.*, Proc. SPIE **3158**, 28 (1997).
[2] N. Piovella, P. Chaix, G. Shvets, and D. A. Jaroszynski, Phys. Rev. E **52**, 5470 (1995).
[3] D. A. Jaroszynski, R. J. Bakker, A. F. G. van der Meer, D. Oepts, and P. W. van Amersfoort, Phys. Rev. Lett. **70**, 3412 (1993).
[4] D. A. Jaroszynski, D. Oepts, A. F. G. van der Meer, and P. Chaix, Nucl. Instrum. Methods Phys. Res. A **407**, 407 (1998).
[5] Oscar G. Calderòn, Takuji Kimura, and Todd I. Smith, Phys. Rev. E **65**, 016504 (2002).
[6] S. Riyopoulos and C. M. Tang, Phys. Fluids **31**, 3387 (1988).
[7] W. J. Wang, G. R. Wang, S. G. Chen, and X. W. Du, Prog. Phys. **15**, 19 (1995).
[8] B. Levush, T. M. Antonsen, A. Bromborsky, Alan Bromborsky, Wei-Ran Lou, and Yuval Carmel, IEEE Trans. Plasma Sci. **20**, 263 (1992).
[9] R. Riyopoulos, IEEE Trans. Plasma Sci. **20**, 360 (1992).
[10] M. I. Petelin, Izv. Vyssh. Uchebn. Zaved., Radiofiz. **28**, 354 (1985).
[11] A. N. Vlasov, G. S. Nusinovich, and B. Levush, Phys. Plasmas **4**, 1402 (1997).
[12] R. W. Lemeke, S. E. Calico, and M. C. Clark, IEEE Trans. Plasma Sci. **25**, 364 (1997).
[13] S. E. Calico and C. S. Scott, Proc. SPIE **2557**, 50 (1995).
[14] H. L. Berk, B. N. Breizman, and M. S. Pekker, Plasma Phys. Rep. **23**, 778 (1997).
[15] J. H. Hao and W. Ding (unpublished).